IEEE INSTRUMENTATION & MEASUREMENT SOCIETY

Received 15 September 2023; revised 21 October 2023; accepted 26 October 2023. Date of publication 14 November 2023; date of current version 6 December 2023. The review of this paper was arranged by Associate Editor Subhas Chandra Mukhopadhyay.

Digital Object Identifier 10.1109/OJIM.2023.3332393

Ultrahigh-Sensitivity Pressure Sensor With Graphene Aerogel Electrodes

EZZAT G. BAKHOUM (Senior Member, IEEE)

Department of Electrical and Computer Engineering, University of West Florida, Pensacola, FL 32514, USA

CORRESPONDING AUTHOR: E. G. BAKHOUM (e-mail: ebakhoum@uwf.edu)

ABSTRACT A new pressure sensor with ultrahigh sensitivity is presented. The sensor is based on the concept of creating a variable supercapacitor that responds to pressure. The sensor consists mainly of a liquid electrolyte and two graphene aerogel electrodes. As pressure is applied to the graphene aerogel electrodes, the liquid electrolyte penetrates in the pores of the electrodes, and a variable supercapacitor is obtained. The sensor is sensitive to pressures of less than 0.1 Pa. Characteristics of the sensor, such as accuracy, nonlinearity, and response time, are fully analyzed.

INDEX TERMS Graphene aerogel, pressure measurement system, pressure sensor, variable supercapacitor.

I. INTRODUCTION AND PRINCIPLE OF OPERATION

GRAPHENE aerogel is the lightest material in existence. It is also a high-strength, high-porosity material. Because it is carbon with a very high internal surface area, graphene aerogel has been used recently as electrode material in supercapacitor applications [1], [2]. This article presents a new type of pressure sensor with very high sensitivity that utilizes graphene aerogel as electrodes. The fundamental idea is to create a *variable supercapacitor* when pressure is applied to the electrodes. Fig. 1 shows this fundamental principle.

As shown in Fig. 1, two graphene aerogel electrodes are placed inside a plastic tube. The space between the electrodes is filled with a supercapacitor electrolyte (in the present application, the electrolyte is propylene carbonate, in which the ionic salt tetraethylammonium tetrafluoroborate, or TEA/BF4, is dissolved). Because carbon is super-hydrophobic, the electrolyte does not penetrate inside the pores of the electrodes when pressure is absent [Fig. 1(a)]. Hence, in the absence of pressure, the capacitance between the two graphene aerogel electrodes is approximately equal to zero. As pressure is applied to one or both electrodes [Fig. 1(b)], the electrolyte penetrates inside the pores of the two electrodes, and a supercapacitor structure is obtained. Because the structure in Fig. 1(b) is a variable supercapacitor, the sensor is extremely sensitive to minute variations in pressure. The prototype that was assembled by the author can detect a pressure of less than 0.1 Pa and has a maximum detection range of 10 Pa.

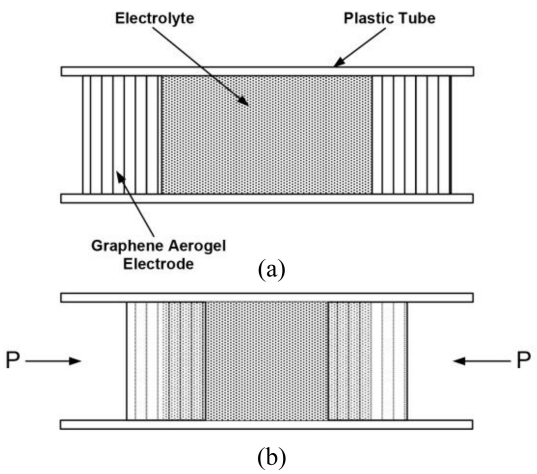

FIGURE 1. Fundamental principle of the pressure sensor with graphene aerogel electrodes. (a) No pressure is applied to the electrodes. (b) Pressure is applied, and hence the liquid electrolyte penetrates in the internal pores of the electrodes, creating a supercapacitor structure.

Fig. 2 shows a photograph of the components of the prototype that was assembled by the author (the liquid electrolyte is not shown).[1]

The recent literature contains numerous references that describe innovative pressure sensors [3], [4], [5], [6], [7], [8], [9], [10], [11], [12], [13], [14], [15], [16], [17], [18],

1. Because graphene aerogel is super-hydrophobic, it was found that the electrolyte does not leak out of the sensor during normal operation. In addition, because propylene carbonate has a very low volatility rate, the sensor has a long shelf life.

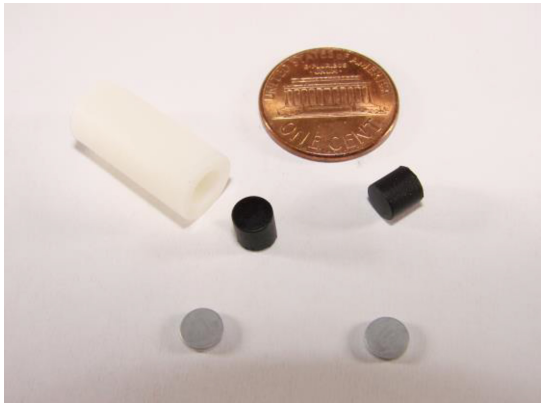

FIGURE 2. Components of the sensor. The two black cylinders are the graphene aerogel electrodes. One U.S. penny is shown in the figure for size comparison.

[19], [20], [21], [22], [23]. Those sensors usually use either the principle of piezoresistivity [3], [4], [5], [6], [7], [8], [9], [10], [12], [14], [15], [17], [21] (see Appendix A for performance parameters) or capacitance variation [11], [13], [16], [18], [19], [20], [22], [23] (see Appendix A). The advantage of the new sensor introduced in this article is the excellent sensitivity to very low pressures (0.1–10 Pa).

This article is organized as follows. Section II gives the theory of the new pressure sensor with graphene aerogel electrodes. Section III presents the experimental results. Section IV describes an integrated pressure measurement system that consists of the new sensor and an Arduino circuit board. Section V contains the conclusions.

II. THEORY OF OPERATION

A. PENETRATION DEPTH OF THE ELECTROLYTE INSIDE THE GRAPHENE AEROGEL ELECTRODE

The penetration of fluids in porous media is generally described by Darcy's law [24]

$$q = -\frac{k}{\mu l}\Delta p \tag{1}$$

where q (m/s) is the instantaneous flux, k (m^2) is the permeability of the porous medium, μ (Pa s) is the dynamic viscosity of the fluid, and Δp (N/m^2) is the pressure drop over a given distance l. The capillary pressure inside the porous medium is given by the Young–Laplace equation [24]

$$\Delta p = \frac{2\gamma\cos\theta}{r} \tag{2}$$

where γ (N/m) is the surface tension of the fluid, θ is the contact angle, and r is the radius of the capillary pore. Equation (1) can now be rewritten as

$$q = \Phi\frac{dl}{dt} = \frac{k}{\mu}\frac{2\gamma\cos\theta}{rl} \tag{3}$$

where Φ (dimensionless) is the porosity of the solid medium. The penetration depth l inside the porous medium can be obtained by integrating (3), resulting in

$$l = \sqrt{\frac{4k}{\mu\Phi}\frac{\gamma\cos\theta}{r}\,t} = \sqrt{\frac{2k}{\mu\Phi}\,\Delta p\,t}. \tag{4}$$

The parameter t in the above equation is the settling time (or time required for the penetration depth to reach a steady state) and must be determined experimentally.

B. CAPACITANCE OF THE SUPERCAPACITOR AS FUNCTION OF APPLIED PRESSURE

The volume of the electrode that will be immersed in the liquid electrolyte is equal to al, where a is the cross-sectional area of the electrode (see Fig. 1). The internal surface area of the graphene aerogel material that is immersed in the electrolyte, A, will be given by

$$A = \frac{al}{1(m^3)} \times I \tag{5}$$

where I is the internal surface area per cubic meter of the graphene aerogel material. The capacitance of a supercapacitor is given by the following expression [25]:

$$C = \frac{1}{2}\frac{\epsilon_0\epsilon_r A}{d} \tag{6}$$

where ϵ_0 is the permittivity of free space, ϵ_r is the relative permittivity of the electrolyte, A is the internal surface area of the electrode material that is immersed in the electrolyte, and d is the distance between the surface of the electrode and an ion in the electrolyte. From (5) and (6), we have

$$C = \frac{1}{2}\frac{\epsilon_0\epsilon_r}{d}\,al\,I. \tag{7}$$

Now, from (7) and (4), we have

$$C = \frac{1}{2}\frac{\epsilon_0\epsilon_r}{d}\,aI\left(\sqrt{\frac{2k}{\mu\Phi}\,\Delta p\,t}\right). \tag{8}$$

Solving the above equation for the pressure drop Δp gives

$$\Delta p = \frac{2\mu\Phi}{kt}\left(\frac{Cd}{\epsilon_0\epsilon_r aI}\right)^2. \tag{9}$$

The following are the physical constants of the liquid electrolyte and the graphene aerogel electrodes.

1) $\mu = 2.5 \times 10^{-3}$ Pa s [26].
2) Φ is the ratio of the pore volume (volume of all the pores in a sample of graphene aerogel) to the total volume of the sample. Given that the pore diameter in graphene aerogel is approximately equal to 500 nm [27], we find that $\Phi \approx 2.6 \times 10^{-7}$.
3) $k = 3 \times 10^{-14}$ m^2 [28].
4) $d \approx 1$ nm in supercapacitors [25].
5) $\epsilon_r \approx 1$ in supercapacitors [25].
6) $I \approx \$\ 416\,000$ m^2 [29].
7) Diameter of the graphene aerogel electrode = 5 mm.

By substitution with the above parameters in (9), we find

$$\Delta p = 18.72 \times 10^6\ \frac{C^2}{t}. \tag{10}$$

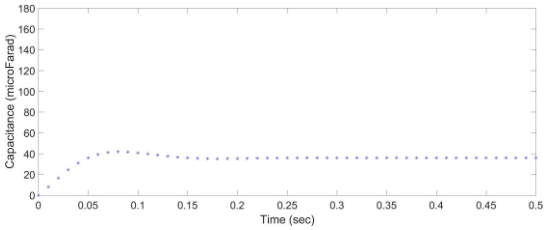

FIGURE 3. Measured capacitance between the electrodes as a function of time, for an applied pressure of 0.1 Pa.

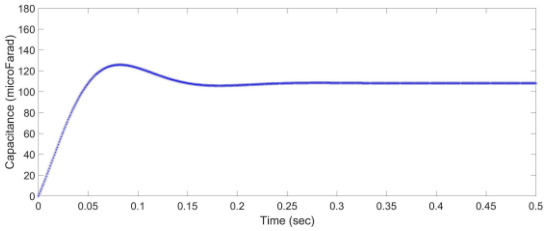

FIGURE 4. Measured capacitance between the electrodes as a function of time, for an applied pressure of 0.9 Pa.

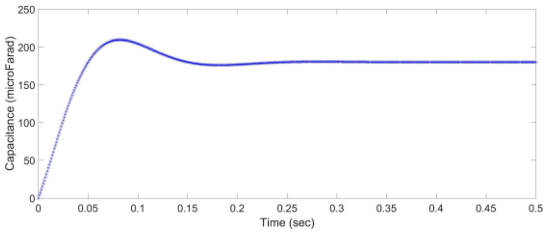

FIGURE 5. Measured capacitance between the electrodes as a function of time, for an applied pressure of 2.5 Pa.

TABLE 1. Error in calculated pressure as a function of the actual applied pressure.

Measured Capacitance	Calculated Pressure	Actual Pressure	Error
36.45 μF	0.0995 Pa	0.1 Pa	0.5%
182.10 μF	2.483 Pa	2.5 Pa	0.7%
363.24 μF	9.880 Pa	10 Pa	1.2%

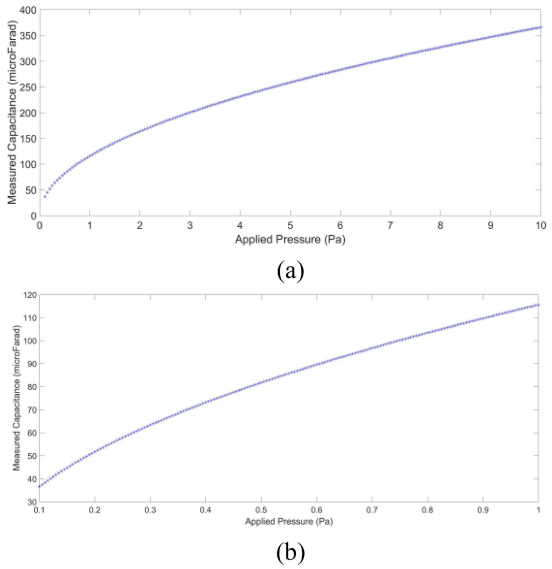

FIGURE 6. (a) Measured capacitance (in micro-Farad) as a function of the applied pressure (in Pa) at room temperature. (b) Measured capacitance (in micro-Farad) as a function of the applied pressure (in Pa) at room temperature for the narrow range of 0.1–1 Pa.

III. EXPERIMENTAL RESULTS

A. MEASUREMENT OF THE SETTLING TIME

For the purpose of measuring the settling time (t), the sensor was placed inside a small chamber that is equipped with an air pump. The chamber is also equipped with its own pressure sensor (model A10 by WIKA Instruments, Lawrenceville, GA, USA). The leads that are connected to the graphene aerogel electrodes were connected to a capacitance meter. The output of the capacitance meter was connected with a USB cable to a computer that runs MATLAB (see Fig. 7). For each new incremental value of the pressure inside the chamber, the capacitance was measured in real time and was stored for analysis. Figs. 3–5 show the measured capacitance as a function of time, for an applied pressure of 0.1, 0.9, and 2.5 Pa, respectively.

As Figs. 3–5 show, the settling time (or time that is required for the fluid to reach a steady state inside the graphene aerogel electrode) is approximately 0.25 s, regardless of the final value of capacitance. Equation (10) now becomes

$$\Delta p = 74.88 \times 10^6 \ C^2. \tag{11}$$

B. MEASUREMENT ACCURACY

Table 1 lists a few values for the capacitance measured between the two graphene aerogel electrodes, the pressure calculated from (11), and the actual pressure (measured with the commercial sensor that is attached to the pressure chamber). As can be seen, the error is approximately 0.5% at a pressure of 0.1 Pa and is approximately 1.2% at a pressure of 10 Pa (maximum reading).

It is to be noted that while the size of the pores in graphene aerogel is inconsistent, it was experimentally found that the porosity [the parameter Φ in (9)] tends to be very consistent from sample to sample. This leads to the almost perfect agreement between the pressure given by (11) and the pressure readings of commercially available pressure sensors. (The experiment was repeated with several prototypes that were made by the author, and the readings of the different prototypes were consistent.)

Fig. 6(a) shows several values of the measured capacitance (in micro-Farad) as a function of the applied pressure (in Pa).

Fig. 6(b) is a plot of the measured capacitance as a function of the applied pressure for the narrow range of 0.1–1 Pa. As can be seen from the plot, the ultrahigh sensitivity of the sensor is reflected in the significant range of capacitance variation (from 36 to 115 μF).

Fig. 7 is a photograph that shows the experimental setup: the pressure chamber (BUCO model 100 kPa), the air pump (RYOBI model P747), the capacitance meter (AGILENT model U1701B), and a Windows PC.

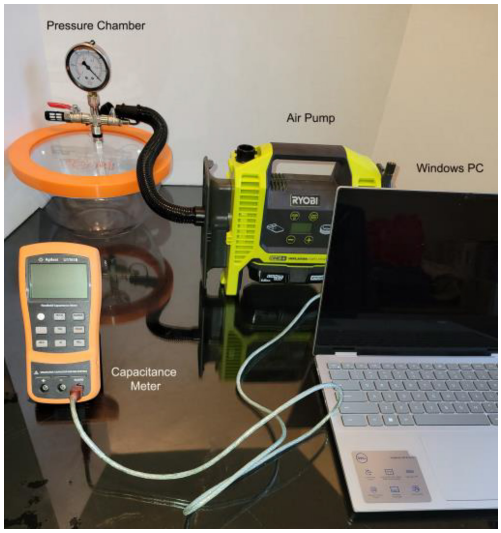

FIGURE 7. Experimental setup: pressure chamber, air pump, capacitance meter, and a Windows PC.

C. NONLINEARITY

The sensor was tested in a variable temperature chamber (BINDER model MK 56). Fig. 8 shows two plots of the measured pressure versus the true applied pressure, at temperatures of −10 °C and +80 °C (the working range, as shown, is 8–10 Pa). As can be seen from the plots, the nonlinearity error is approximately 1.3% of FSO at a temperature of −10 °C and is approximately 4.0% of FSO at +80 °C. (*Notes:* 1) In this application, nonlinearity is the discrepancy between two measurements taken at the same operating point but at different times and 2) the data at room temperature fits between the two data sets of −10 °C and +80 °C.)

To investigate the repeatability of the results in Fig. 8, the testing was repeated several times. The shape of the curves was found to be different in each experiment; however, the nonlinearity error was found to be consistent—specifically, 1.3% of FSO at a temperature of −10 °C and 4.0% of FSO at +80 °C.

D. CAPACITANCE-PRESSURE RELATIONSHIP AT VARIOUS TEMPERATURES

Fig. 9 shows two plots of the measured capacitance as a function of the applied pressure, at temperatures of −10 °C and +80 °C.

As can be concluded from Fig. 9, the effect of the temperature on the capacitance measurement is not significant. This is due to the fact that the settling time (or time that is required for the liquid electrolyte to reach a steady state inside the graphene aerogel electrode) is approximately 0.25 s regardless of the final value of capacitance, as pointed out in Section III above. Explained differently, it takes a finite amount of time for the ions in the electrolyte to reach the internal surface of the graphene aerogel electrode—a time after which the capacitance value will be the same regardless of temperature.

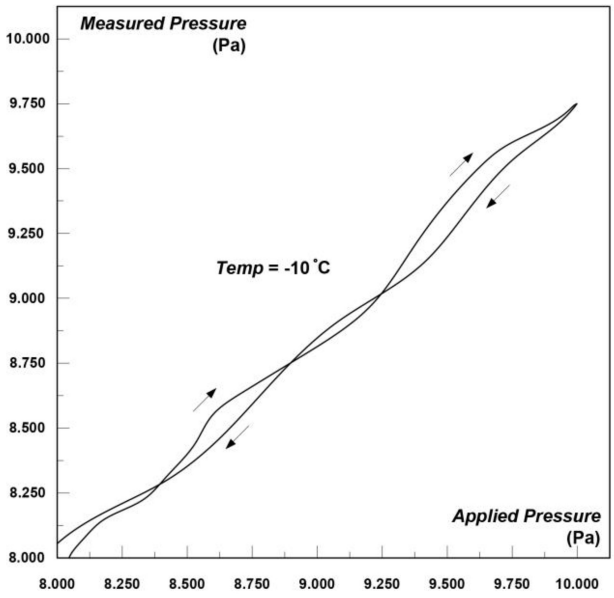

(a)

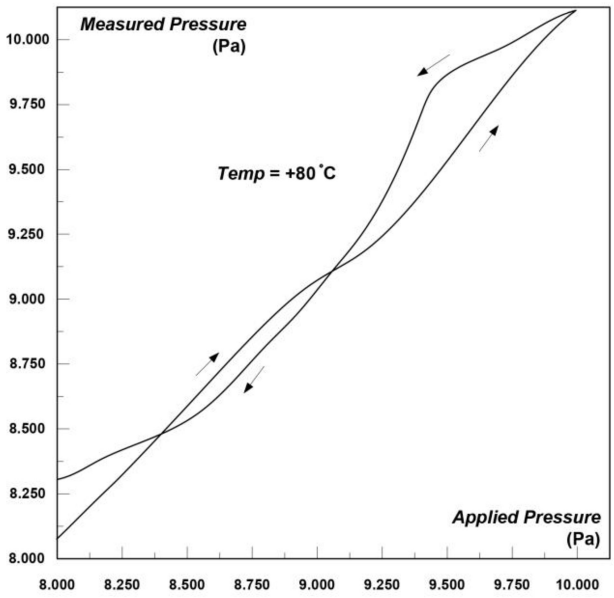

(b)

FIGURE 8. Measured pressure versus true applied pressure, at (a) −10 °C and (b) +80 °C.

IV. INTEGRATED SENSOR—ARDUINO PRESSURE MEASUREMENT SYSTEM

The sensor can be easily integrated with an Arduino circuit board to form a complete (stand alone) pressure measurement system. As shown in Fig. 10, the sensor is connected between the ground terminal and the analog input terminal of the Arduino board. The sensor is essentially a variable

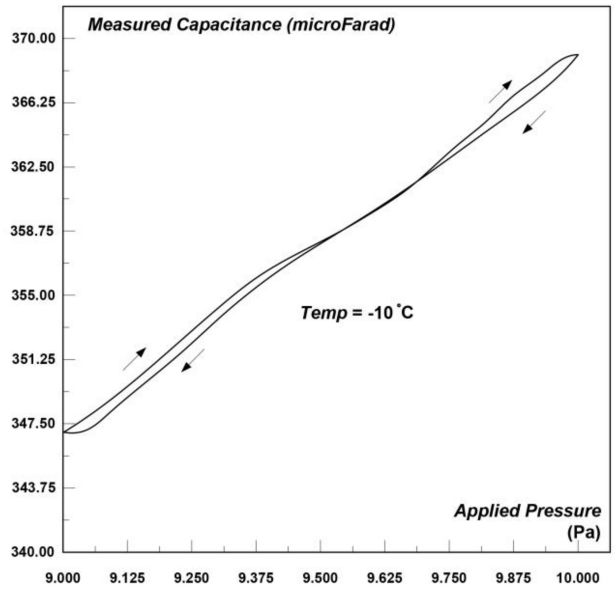

(a)

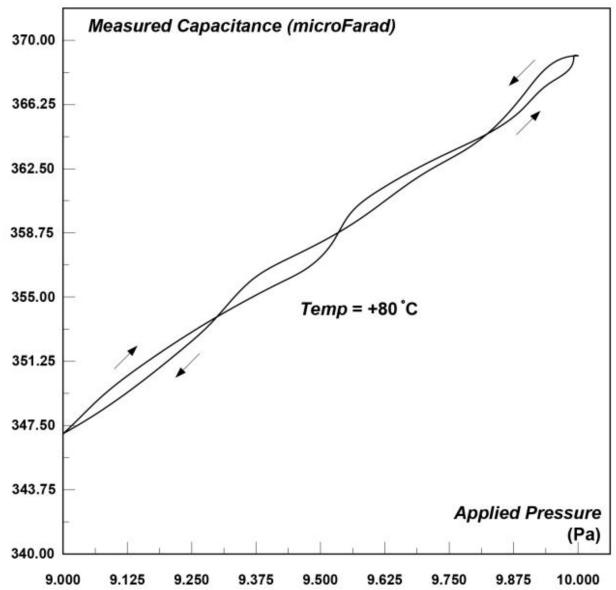

(b)

FIGURE 9. Capacitance as a function of the applied pressure, at (a) −10 °C and (b) +80 °C.

capacitor, and the capacitance can be measured by further connecting the sensor to a resistor with a known value, as shown in the figure. The C code running on the Arduino board measures the time taken for the capacitor's voltage to reach 63.2% of the supply voltage (Vcc). This time is the time constant τ of the RC circuit. By dividing the time constant by the ohmic value of the resistor, the value of the capacitance C is obtained. The C code running on the Arduino board finally calculates the pressure (in Pa) from (11) and displays the pressure on an LCD display that is attached to the board.

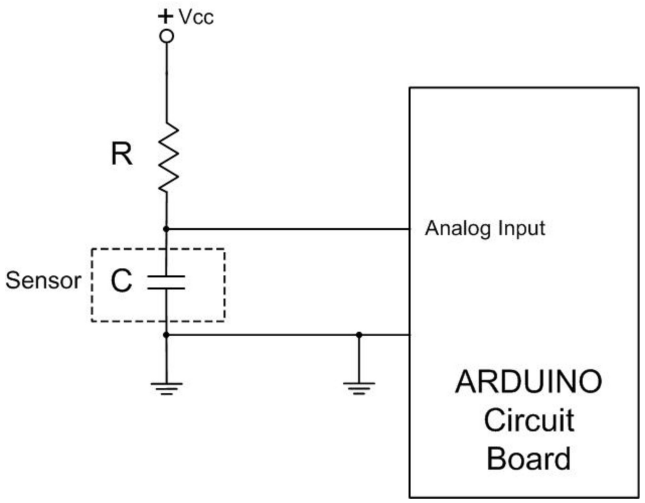

FIGURE 10. Integrated sensor—Arduino pressure measurement system.

TABLE 2. Comparison of the new sensor to existing state-of-the-art pressure sensors.

Type of Sensor	Measurement Range	Nonlinearity	Application
Capacitive (references [11,13,16,18,19,20, 22,23])	few kPa to several kPa	0.5% FSO or higher	Detection of finger pressure, measurement of vacuum pressure
Piezoresistive (references [3,4,5,6,7,8,9,10,12 ,14,15,17,21])	several kPa	0.5% to 5% FSO	Wide variety of applications (biological, instrumentation , etc.)
Present sensor	0.1 Pa to 10 Pa	1.3% to 4% FSO	Medical instrumentation , clean rooms, R&D

V. CONCLUSION

A pressure sensor with ultrahigh sensitivity was presented. The new sensor consists of a liquid electrolyte and two graphene aerogel electrodes. This structure results in a variable supercapacitor when pressure is applied to the electrodes. The sensor can easily measure extremely low pressures (less than 0.1 Pa). The error in measurement is approximately 0.5% at a pressure of 0.1 Pa and is approximately 1.2% at the maximum reading of 10 Pa. The nonlinearity error is approximately 1.3% of FSO at a temperature of −10 °C and is approximately 4.0% of FSO at a temperature of +80 °C. The sensor will be useful in applications, such as medical instrumentation, manufacturing, and clean rooms, in addition to a wide variety of research and development applications.

APPENDIX A

Table 2 presents points of comparison between the performance of the new sensor presented in this article to the performance/characteristics of state-of-the-art pressure

FIGURE 11. Modified digital manometer reading the static pressure in an HVAC system.

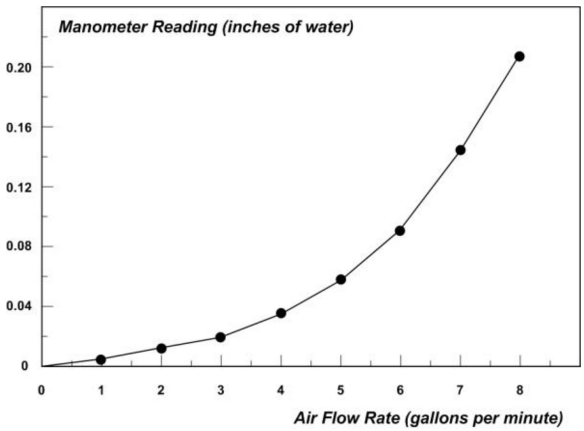

FIGURE 12. Manometer reading versus air flow rate.

sensors [3], [4], [5], [6], [7], [8], [9], [10], [11], [12], [13], [14], [15], [16], [17], [18], [19], [20], [21], [22], [23].

APPENDIX B

The following is a description of a practical application of the new sensor: a version of the sensor that is capable of measuring up to 100 Pa was developed. The sensor was then integrated with an Arduino circuit board, as shown in Fig. 10. The integrated system was then used to replace the electronic circuit board in a digital manometer. The modified digital manometer is shown in Fig. 11 (only the LCD was not replaced). As the figure shows, the manometer is reading the static pressure in an HVAC system.

Fig. 12 shows a plot of the reading of the manometer (converted to inches of water) versus the air flow rate in gallons per minute. As expected, the manometer reading is proportional to the square of the air flow rate.

REFERENCES

[1] J. S. Shaikh et al., "The implementation of graphene-based aerogel in the field of supercapacitor," *Nanotechnology*, vol. 32, no. 36, pp. 1–23, 2021.
[2] Z. Yu, M. McInnis, J. Calderon, S. Seal, L. Zhai, and J. Thomas, "Functionalized graphene aerogel composites for high-performance asymmetric supercapacitors," *Nano Energy*, vol. 11, pp. 611–620, Jan. 2015.
[3] L. Gao et al., "An ultrahigh sensitive paper-based pressure sensor with intelligent thermotherapy for skin-integrated electronics," *Nanomaterials*, vol. 10, no. 12, pp. 25–36, 2020.
[4] P. Nicolay and M. Lenzhofer, "A wireless and passive low-pressure sensor," *Sensors*, vol. 14, no. 2, pp. 3065–3076, 2014.
[5] C. Xiang, Y. Lu, C. Cheng, J. Wang, D. Chen, and J. Chen, "A resonant pressure microsensor with a wide pressure measurement range," *Micromachines*, vol. 12, no. 4, 2021, Art. no. 382.
[6] D. Gräbner, M. Tintelott, G. Dumstorff, and W. Lang, "Low-cost thin and flexible screen-printed pressure sensor," *Proc. Eurosensors*, 2017, pp. 3–6.
[7] S. B. Subramanya, B. Pavithra, M. M. Nayak, and M. G. A. Prasad, "Realization of a micro composite based pressure sensor: Its performance study for linearity, hysteresis and sensitivity," *SN Appl. Sci.*, vol. 1, 2019, Art. no. 1737.
[8] F. E. Fajingbesi, A. W. Azman, Z. Ahmad, R. F. Olanrewaju, M. I. Ibrahimy, and Y. M. Mustafah, "Low cost piezoresistive pressure sensor matrix for pressure ulcer prevention and management," in *Proc. IEEE 7th Int. Conf. Mechatronics Eng. (ICOM)*, 2019, pp. 1–4.
[9] X. Huang and D. Zhang, "High sensitive and linear pressure sensor for ultra-low pressure measurement," *Procedia Eng.*, vol. 87, 2014, pp. 1202–1205.
[10] R. Tang et al., "Flexible pressure sensors with microstructures," *Nano Sel.*, vol. 2, no. 10, pp. 1874–1901, 2021.
[11] L. A. Kurup, C. M. Cole, J. N. Arthur, and S. D. Yambem, "Graphene porous foams for capacitive pressure sensing," 2021, *arXiv:2111.06052*.
[12] H. Tian et al., "A graphene-based resistive pressure sensor with record-high sensitivity in a wide pressure range," *Sci. Rep.*, vol. 5, 2015, Art. no. 8603.
[13] R. Li et al., "Research progress of flexible capacitive pressure sensor for sensitivity enhancement approaches," *Sens. Actuators A, Phys.*, vol. 321, no. 15, 2021, Art. no. 112425.
[14] J. Sosa, J. A. Montiel-Nelson, R. Pulido, and J. C. Garcia-Montesdeoca, "Design and optimization of a low power pressure sensor for wireless biomedical applications," *J. Sensors*, vol. 2015, 2015, Art. no. 352036.
[15] Z. Kordrostami, K. Hassanli, and A. Akbarian, "MEMS piezoresistive pressure sensor with patterned thinning of diaphragm," *Microelectron. Int.*, vol. 37, no. 3, pp. 147–153.
[16] Bijender and A. Kumar, "Flexible and wearable capacitive pressure sensor for blood pressure monitoring," *Sens. Bio-Sens. Res.*, vol. 33, Aug. 2021, Art. no. 100434.
[17] T. Jeong, "Theoretical and linearity analysis for pressure sensors and communication system development," *Int. J. Distrib. Sensor Netw.*, vol. 10, no. 9, 2014, Art. no. 902976.
[18] M. R. Buyong, N. A. Aziz, and B. Y. Majlis, "Characterization and optimization of seals-off for very low pressure sensors (VLPS) fabricated by CMOS MEMS process," *Adv. Mater. Res.*, vol. 74, pp. 231–234, Jun. 2009.
[19] E. Pritchard, M. Mahfouz, B. Evans, S. Eliza, and M. Haider, "Flexible capacitive sensors for high resolution pressure measurement," in *Proc. IEEE Sensors Conf.*, 2008, pp. 1484–1487.
[20] L. Yang et al., "Wearable pressure sensors based on MXene/tissue papers for wireless human health monitoring," *ACS Appl. Mater. Interfaces*, vol. 13, no. 50, pp. 60531–60543, 2021.
[21] A. M. Almassri et al., "Pressure sensor: State of the art, design, and application for robotic hand," *J. Sensors*, vol. 2015, Art. no. 846487.
[22] Q. Su et al., "A stretchable and strain-unperturbed pressure sensor for motion interference–free tactile monitoring on skins," *Sci. Adv.*, vol. 7, no. 48, pp. 1–9, 2021.

[23] J. Sun et al., "Low power AlGaN/GaN MEMS pressure sensor for high vacuum applications," *Sens. Actuators A, Phys.*, vol. 314, Oct. 2020, Art. no. 112217.
[24] C. J. Kuijpers, T. A. P. Van Stiphout, H. P. Huinink, N. Tomozeiu, S. J. F. Erich, and O. C. G. Adan, "Quantitative measurements of capillary absorption in thin porous media by the Automatic Scanning Absorptometer," *Chem. Eng. Sci.*, vol. 178, pp. 70–81, Mar. 2018.
[25] B. E. Conway, *Electrochemical Supercapacitors*, New York, NY, USA: Kluwer Acad. Publ., 1999.
[26] E. Tyunina, V. Afanas, and M. Chekunova, "Viscosity and density of solutions of tetraethylammonium tetrafluoroborate in propylene carbonate at different temperatures," *J. Solution Chem.*, vol. 41, pp. 307–317, Jan. 2012.
[27] W. Deng, Q. Fang, X. Zhou, H. Cao, and Z. Liu, "Hydrothermal self-assembly of graphene foams with controllable pore size," *RSC Adv.*, vol. 6, no. 25, pp. 20843–20849, 2016.
[28] S. K. Datta, N. Simhai, S. N. Tewari, J. E. Gatica, and M. Singh, "Permeability of microporous carbon preforms," *Metallurgical Mater. Trans. A*, vol. 27, pp. 3669–3674, 1996.
[29] L. Ren et al., "3D hierarchical porous graphene aerogel with tunable meso-pores on graphene nanosheets for high-performance energy storage," *Sci. Rep.*, vol. 5, Sep. 2015, Art. no. 14229.
[30] J. Vresk, "Methods for improving the accuracy of air flow measurements," U.S. Dept. Energy, Argonne Nat. Lab., Lemont, IL, USA, Rep. ANL/SDP-10; SOLAR/0908-80/70, Sep. 1980. [Online]. Available: https://www.osti.gov/servlets/purl/7045137

EZZAT G. BAKHOUM (Senior Member, IEEE) received the B.S. degree in electrical engineering from Ain Shams University, Cairo, Egypt, in 1986, and the M.S. and Ph.D. degrees in electrical engineering from Duke University, Durham, NC, USA, in 1989 and 1994, respectively.

From 1994 to 1996, he was a Senior Engineer and a Managing Partner with ESD Research, Inc., Research Triangle Park, Durham. From 1996 to 2000, he was a Senior Engineer with Lockheed Martin/L3 Communications, Inc., Camden, NJ, USA. From 2000 to 2005, he was a Lecturer with the Electrical Engineering Department, New Jersey Institute of Technology, Newark, NJ, USA. He is currently a Professor with the University of West Florida, Pensacola, FL, USA.